J. Biomed. Eng. Res.
Vol.26, No.4, 185-191, 2005

Down-Scaled 3D Object for Telediagnostic Imaging Support System

Hang-Sik Shin, Sung-Won Yoon, Jae-Young Kim, Myoungho Lee

Department of Electrical and Electronic Engineering, College of Engineering, Yonsei University
(Received February 2, 2005. Accepted July 25, 2005)

Abstract: In this paper, we proposed a downscaled 3D object technique using medical images for telediagnostic use. The proposed system consisted of downscaling / thresholding processes for building a downscaled 3D object and a process for obtaining 2D images at specific angles for diagnosis support. We used 80 slices of Digital Imaging and Communication in Medicine(DICOM) CT images as sample images and the platform-independent Java language for the experiment. We confirmed that the total image set size and transmission time of the original DICOM image set using a down-scaled 3D object decreased approximately 99% and 98.41%, respectively. With additional studies, the proposed technique obtained from these results will become useful in supporting diagnosis for home and hospital care.

Key words: DICOM, 3D medical image, Image downscaling, Thresholding, E-Health

INTRODUCTION

Although the study of medical service at a remote place, such as telemedicine, developed since the 1970s, limitations of space, time, network bandwidth, and large volume of medical data made it difficult to provide medical service efficiently [1]-[3] (see Table 1). These days, however, technical problems have decreased due to the development of broadband network and improved PC performance, and it has become possible to extend medical service range from hospital/domestic to home/international [4]. Hospital medical imaging system is also actively being diffused with digital imaging developments [5]-[6]. For example, the diffusion rates of PACS (Picture Archiving and Communication System) using hospital intranets and other networks are expected to be 67% of all hospitals in the United State and 60 to 70% in Europe by 2007 . In addition, studies of web-PACS, tele-PACS, satellite-PACS, and portable-PACS using mobile communication systems and devices such as PDAs (Personal Digital Assistant) and cellular phones are also proceeding actively [7]-[10]. There is, however, still a need for technical solutions and supporting methods to transmit data more efficiently and rapidly.

Corresponding Author: Myoungho Lee
Department of Electrical and Electronic Engineering, College of Engineering, Yonsei University, 134 Sinchon-dong, Seodaemun-gu, Seoul, Korea
Tel. (02)2123-4947, FAX. (02) 312-2770
E-mail. mhlee@yonsei.ac.kr

Furthermore, more research is needed on medical image compression, efficient diagnosis support method, and traffic reduction in medical image transmission.

Until now, for better image transfer, researches on image compression methods using JPEG compression [11] and downscaling [12] were carried out, but they have not yet adapted to medical imaging transfer system efficiently. Moreover, the telediagnostic imaging support technique is not suitable for doctor-to-doctor diagnosis support system because medical image size is very large and it is very difficult to extract a 2D sliced image at a specific direction [13]. We developed a downscaled 3D object system that supports transmitting 3D medical images for telediagnostic use, an effective telediagnostic imaging support system which can decrease medical image traffic and produce 2D sliced images at specific directions. We expect that as this system becomes more useful in telemedicine, more related techniques will be developed.

METHODS AND MATERISLS

The main purpose of the proposed system is to build and transmit a down-scaled 3D object for telediagnostic use, allowing reading-client and request-client to transmit object files to each other to support tele-imaging in case of need. The down-scaled 3D object building process is as follows: down-scaling, thresholding, and object building.

A total system flowchart is shown in Figure 1. As shown in the flowchart, the request-client makes a request to the reading-client when a doctor needs help, then the request-client builds and transmits a downscaled 3D object through downscaling, thresholding, and object building processes if the reading-client accepts it. The reading-doctor performs 3D object transformations and finds a diagnostic angle with the downscaled 3D object after receiving the object file from the reading-doctor. Finally, the reading-doctor makes a diagnosis with the sectioned 2D image from the diagnostic angle data.

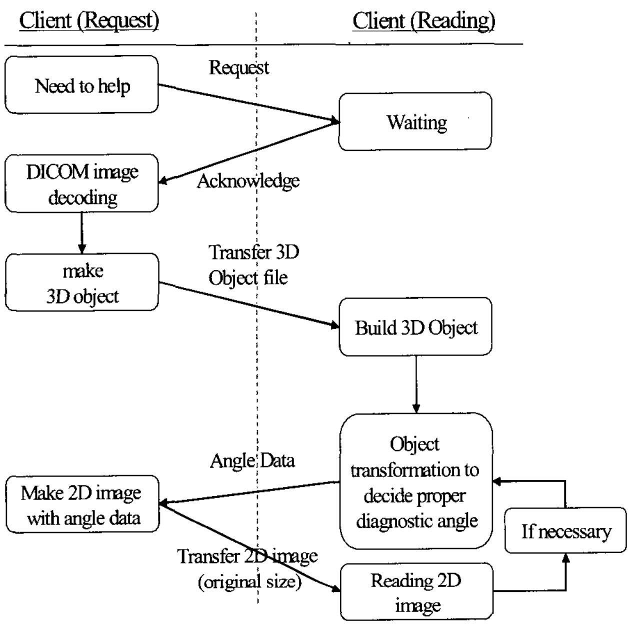

Fig. 1. A total system flowchart of the proposed system

DICOM Image Acquisition and Down-Scaling

For the process, we must analyze the DICOM file and obtain a 2D medical image. In the first step, we analyze the DICOM header to obtain image information. DICOM 2D image can be represented after the header analysis because the DICOM header contains patient information, device information, and image information for all different images. In this paper, we use CT images and the Hounsfield Unit (HU) for CT image representation. The HU of a tissue varies according to the density of the tissue, with denser tissues having higher numbers. The HU range is between +1000 HU and -1000 HU for bone and air respectively. Recently, the scale has been extended to +4000 for bone imaging.

We perform the downscaling process after the 2D image representation. The down-scaling process is a very simple method, one of choosing even or odd rows/columns of the original 2D image, and this method efficiently reduces processing time. The down-scaling process is shown in Figure 2.

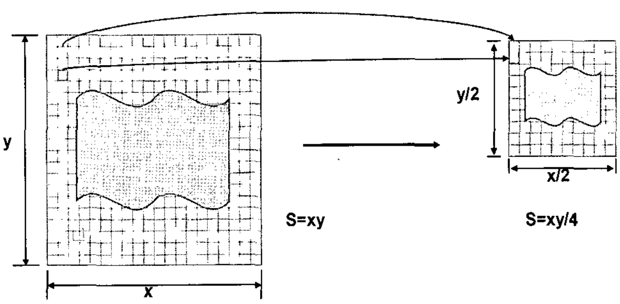

Fig. 2. 2D DICOM Image down-scaling

Table 1. Medical image sizes

Modality	Image Dimension	Gray Level (Bits)	Average Size/Exam
Nuclear medicine (PET and SPECT)	128 × 128	8 or 16	1-2 Mbytes
Magnetic resonance imaging (MRI)	256 × 256	12	8 Mbytes
Ultrasound (US)	512 × 512	8	5-8 Mbytes
Digital subtraction anglography (DSA)	512 × 512	8	4-10 Mbytes
Computed Tomography (CT)	512 × 512	12	20 Mbytes
Digitized electronic Microscophy (DEM)	512 × 512	8	Varies
Digitized Color Microscophy	512 × 512	24	Varies
Digitized X-ray	2048 × 2048	12	8 Mbytes
Computed Radiography (CR)	2048 × 2048	12	8-32 Mbytes
Digitized Mamography	4096 × 4096	12	32 Mbytes (one image)

Thresholding with HU Value

After image downscaling, we perform thresholding with the proper HU value of images. We obtain only the surface or desired pixel data through the thresholding process. It is very important to define a proper threshold because the down-scaled 3D object needs only surface images and smaller data size. Thresholding technique is also a very simple process like the down-scaling technique: a fixed threshold value is set, and if a pixel value is below the fixed threshold, it is set to 0. The '0' value is disregarded when the object file is created.

Building a Downscaled 3D Object

A down-scaled 3D object can be made by rearranging each 2D image that was obtained through the down-scaling and thresholding processes. In composing the 3D object, we use down-scaled 2D images and rearrange each slice with a slice interval which is half the thickness of the original slice (see Figure 3). Slice thickness is the value of physical thickness of each slice, and we assume that a slice interval is the distance between each slice for the computerized image. With these methods, the down-scaled object length in the z-axis decreases by 1/2 as it does in the x and y-axes. Therefore, in accordance with the threshold, the total size of 3D object becomes less than 1/4 of the original image set size. The entire process of building a down-scaled 3D object is shown in Figure 4.

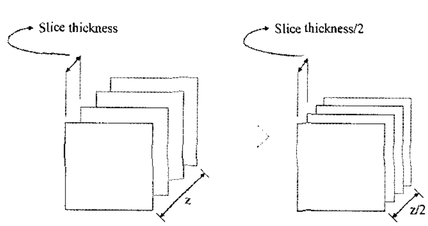

Fig. 3. Decrease of z-axis length due to change in slice thickness for DICOM 3D object

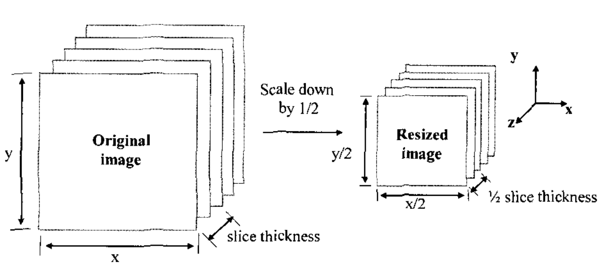

Fig. 4. Summary of building down-scaled 3D object

Obtaining a 2D Image with Specific Angle Data

Once 3D object building is completed, a request-client transmits the down-scaled 3D object to a reading-client. Then a reading-doctor performs object transformations with the down-scaled 3D object, which is received from a request-client, to obtain the diagnostic angle. The process for obtaining rotational angle data is shown in Figure 5.

Rotational angle can be obtained from the shifting of reference point from A(0,0,1) to A'(x,y,z) with object transformation. As shown in Figure 5, a rotational angle is obtained at every plane, and the angles are as follows: θx from y-z plane, θy from z-x plane, and θz from x-y plane. We can obtain each rotational angle by applying the cosine law after we get an orthogonal projection on each plane of A', Ax, Ay, and Az. We obtain the rotational angle data with equations (1)-(3)

$$\theta_x = \cos^{-1}\frac{z}{\sqrt{y^2+z^2}} \quad (1)$$

$$\theta_y = \cos^{-1}\frac{z}{\sqrt{x^2+z^2}} \quad (2)$$

$$\theta_z = \cos^{-1}\frac{x}{\sqrt{x^2+y^2}} \quad (3)$$

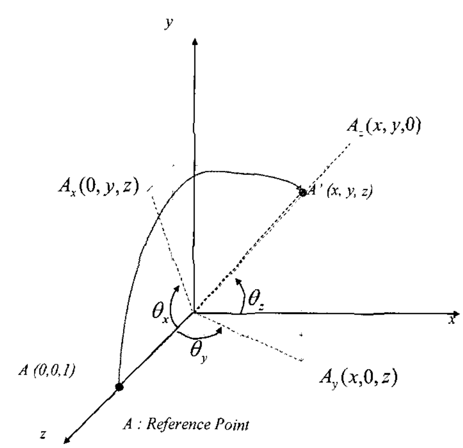

Fig. 5. Rotational angles

Rotational angle information is sent to a request-doctor to obtain the 2D image. For diagnostic use, we are able to acquire the 2D image with the rotational angle information from the original image set. Transform matrices for obtaining the 2D image are shown in equations (4)-(6), and Figure 6 shows the transformation of each slice for obtaining the 2D image.

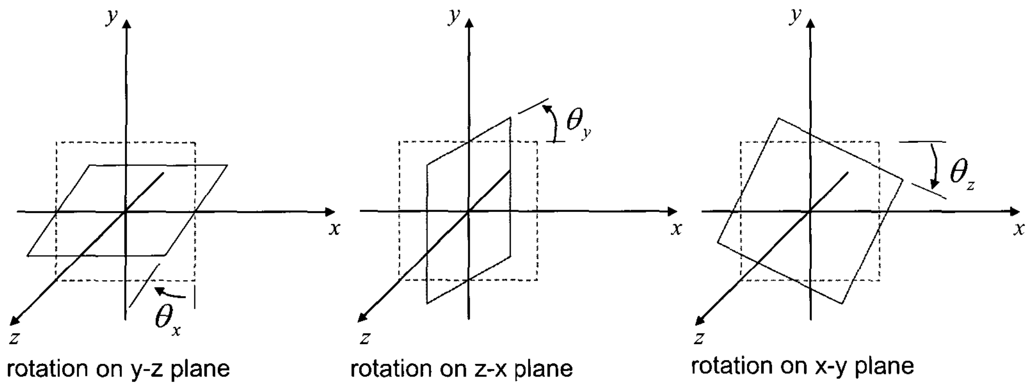

Fig. 6. Transformation of plane for sectioned 2D image

$$T = T_x \times T_y \times T_z \tag{4}$$

$$\begin{bmatrix} t_{11} & t_{12} & t_{13} \\ t_{21} & t_{22} & t_{23} \\ t_{31} & t_{32} & t_{33} \end{bmatrix} = \begin{bmatrix} 1 & 0 & 0 \\ 0 & \cos\theta_x & -\sin\theta_x \\ 0 & \sin\theta_x & \cos\theta_x \end{bmatrix} \times \begin{bmatrix} \cos\theta_y & 0 & \sin\theta_y \\ 0 & 1 & 0 \\ -\sin\theta_y & 0 & \cos\theta_y \end{bmatrix} \times \begin{bmatrix} \cos\theta_z & -\sin\theta_z & 0 \\ \sin\theta_z & \cos\theta_z & 0 \\ 0 & 0 & 0 \end{bmatrix} \tag{5}$$

$$\begin{bmatrix} a_{11} & a_{12} & a_{13} \\ a_{21} & a_{22} & a_{23} \\ \vdots & \vdots & \vdots \\ a_{5111} & a_{5112} & a_{5113} \\ a_{5121} & a_{5122} & a_{5123} \end{bmatrix} \times \begin{bmatrix} t_{11} & t_{12} & t_{13} \\ t_{21} & t_{22} & t_{23} \\ t_{31} & t_{32} & t_{33} \end{bmatrix} = \begin{bmatrix} b_{11} & b_{12} & b_{13} \\ b_{21} & b_{22} & b_{23} \\ \vdots & \vdots & \vdots \\ b_{5111} & b_{5112} & b_{5113} \\ b_{5121} & b_{5122} & b_{5123} \end{bmatrix} \tag{6}$$

EXPERIMENT AND RESULTS

In this experiment, we used 80 slices of 16-bit gray-scale DICOM CT images and Java Language for its platform-independent characteristics. The CT-scan images of the cranium were stored in 512 x 512 pixels, with a pixel size of 0.5 mm x 0.5 mm and slice thickness of 3.0 mm in DICOM format. The scan device was PQ 5000 of Picker International. A total number of 80 slices was obtained to define the whole cranium. The CT images were used for subsequent image processing and analysis. The CT gray value of bone (trabecular and compact) was between -1024(i.e. non-bone) and 3071(i.e. cortical bone). The process for building the down-scaled 3D object consisted of extracting 2D images through DICOM header analysis, down-scaling, thresholding, and then building the 3D object. Furthermore, the transformation of 3D object and obtainment of rotational angle at a reading-doctor were also included in this process.

Obtaining DICOM 2D Images

We calculate the HU value first and then perform other calculations because the HU is used as a reference in the CT case. To obtain the HU value from the pixel value which is included in the DICOM file, because an HU value has 12-bits but the obtained pixel data of a 16-bit gray-scale image have pixel values between 0 and 65535, we take only 12-bits from the 16-bits of data in the recorded platform, little-endian or big-endian. We obtain the HU value with the former process in 2's compliment. Image presentation is made possible by adjusting the contrast and brightness with the window level and window width which are recorded in the DICOM header. The HU value of the experimental image set is shown in Figure 7. The average HU value is 0 HU, standard deviation is 1183 HU, and the HU range is between -1024 HU and 3071 HU in this case.

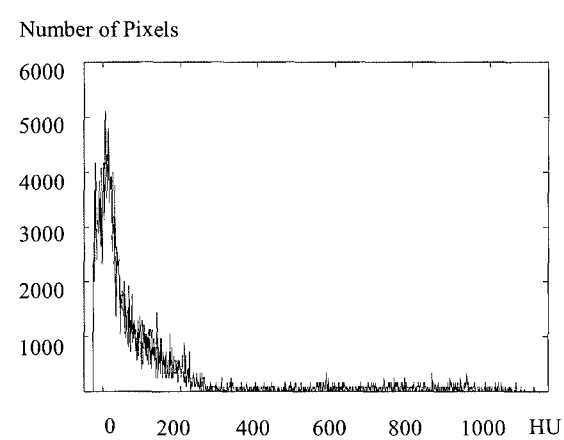

Fig. 7. Hounsfield Unit(HU) in experimental image

Image Downscaling and Thresholding

Figure 8 shows the down-scaled 2D image acquisition process for the 20th, 40th, and 60th DICOM slice images with threshold 600 HU, using the thresholding and down-scaling processes.

Figure 9 shows the sliced 2D image changes in accordance with threshold 10 HU, 50 HU, 150 HU, 300 HU, and 600 HU from the original image. Since threshold means pixel value, a large threshold is more useful in extracting contour images rather than a relatively small threshold. We can view only the cranium images by increasing threshold values in this experiment.

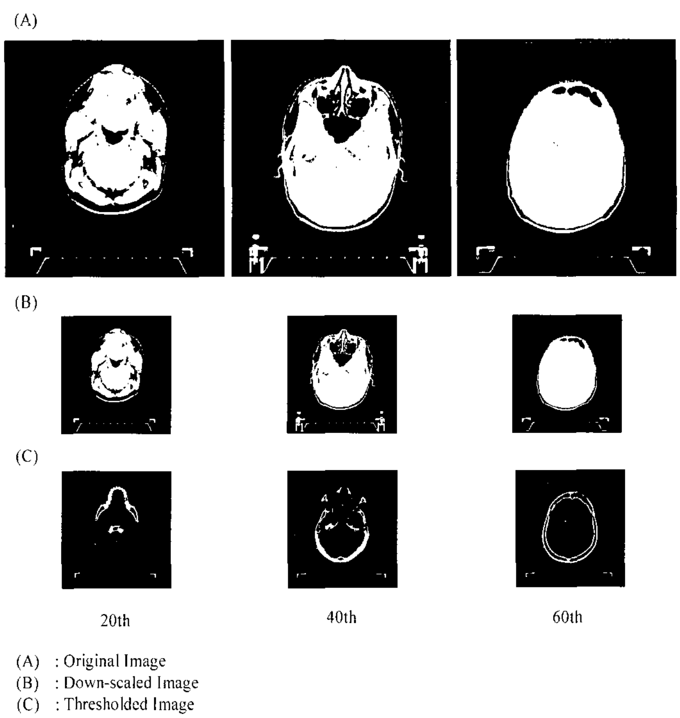

Fig. 8. Image processing for down-scaled 2D images

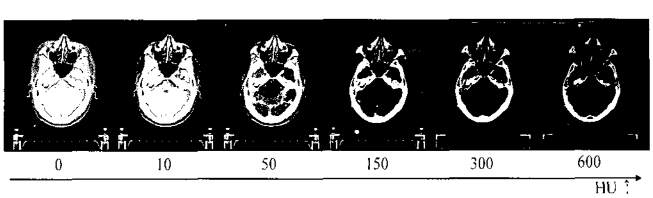

Fig. 9. 2D images with various HU values

Building a Downscaled 3D object

We build a down-scaled 3D object with the down-scaled 2D images by rearranging all slices and confirm that surface pixels change with different thresholds. Low value pixels which represent skin are removed first and high value pixels which represent bones are removed later. There was no problem with identifying the whole shape of the 3D object. The images of the 3D object built from the obtained down-scaled 2D images are shown in Figure 10.

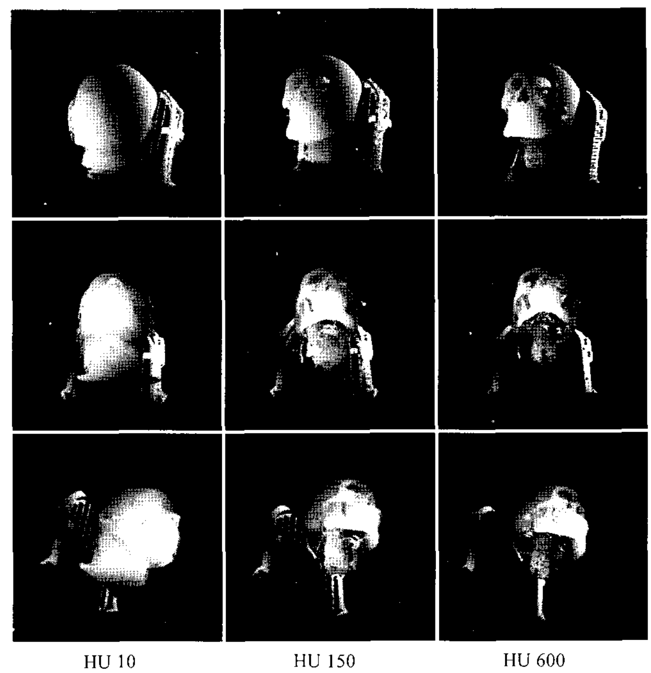

Fig. 10. Down-scaled 3D object with various HU values

Comparison of Data Size and Transmission Time Decrease with Down-Scaled 3D Object

Decrease of down-scaled 3D object file size at each threshold is shown in Table 2. A comparison of file size is made between a 3D object which is made of original images and one made of down-scaled images, between a non-compressed file and a compressed file. The compression method uses the lossless compression technique of Zip library in JAVA.

Table 3 shows that the image transmission time has been decreased. We considered only the compressed case and measured each threshold value in measuring transmission time.

Table 2. Comparison of data size with various thresholds

Object size	Condition	Original	10 HU	50 HU	150 HU	300 HU	600 HU
512 x 512	Not compressed	40.30 MB (A)	118.00 MB	75.00 MB	39.50 MB	30.30 MB	17.50 MB
	/ (A) * 100	-	292.80 %	186.10 %	98.02 %	75.19 %	43.42 %
	Compressed	20.70 MB (B)	9.99 MB	6.51 MB	3.45 MB	2.68 MB	1.60 MB
	/ (B) * 100	-	48.26 %	31.45 %	16.67 %	12.95 %	7.23 %
	/ (A) * 100	51.37 %	24.79 %	16.15 %	8.56 %	6.65 %	3.97 %
256 x 256	Not compressed	10.10 MB (C)	28.50 MB	18.10 MB	9.53 MB	7.31 MB	4.24 MB
	/ (C) * 100	-	282.18 %	179.21 %	94.36 %	72.38 %	41.98 %
	/ (A) * 100	25 %	70.72 %	44.91 %	23.65 %	18.14 %	10.52 %
	Compressed	5.20 MB (D)	2.38 MB	1.56 MB	846 KB	658 KB	401KB
	/ (D) * 100	-	45.77 %	30.00 %	16.27 %	12.65 %	7.71 %
	/ (A) * 100	12.84 %	5.91 %	3.88 %	2.10 %	1.63 %	1.00 %

Table 3. Comparison of transmission time with various thresholds

Object size	Condition	10 HU	50 HU	150 HU	300 HU	600 HU
512 x 512	Compressed	174.62 sec	108.92 sec	57.05 sec	44.31 sec	26.29 sec
	/ (A) * 100	48.57 %	30.30 %	15.87 %	12.33 %	7.31 %
256 x 256	Compressed	34.29 sec	25.67 sec	13.02 sec	10.11 sec	5.71 sec
	/ (A) * 100	9.54 %	7.14 %	3.62 %	2.81 %	1.59 %

*Original Image set transfer time (80 slices image) : 359.49 sec (A)
**Average transfer time : 63.63 kbps
**Standard deviation : 14.98 kbps

Obtaining 2D Slice Image with Diagnostic Angle

We obtained a sliced 2D image at a specific angle with the rotated plane derived from the rotational angle of 3D object. In Figure 11, images in each column represent a 3D object and a section image with a specific angle. The first column images are not rotated, the second column images are rotated 90 degrees on y-axis, and the third row images are rotated 90 degrees on x-axis.

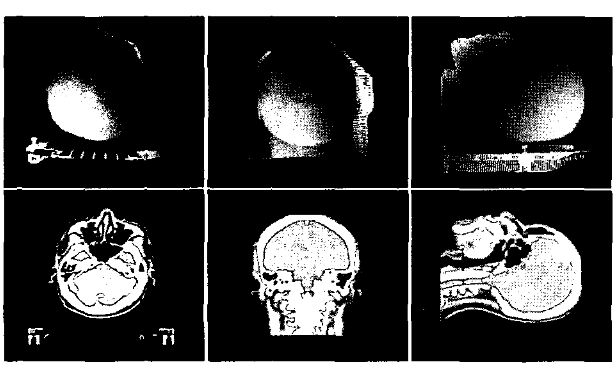

Not rotated | rotation of 90 degrees around the x-axis | rotation of 90 degrees around the y-axis

Fig. 11. 2D images with rotational angles

DISCUSSION AND CONCLUSION

The core techniques of this paper are the extraction technique of 2D image through DICOM header analysis, the down-scaled 3D object building technique using thresholding and down-scaling, and the 2D sliced image acquisition technique. The results of this paper are as follows:

1) The total image size using the proposed down-scaled 3D object technique, when compared with the original image size, decreased to 70.72 %, 44.91 %, 23.65 %, 18.14 %, and 10.52 % under normal conditions and decreased to 5.92 %, 3.88 %, 2.10 %, 1.63 %, and 1.00 % under compressed conditions for the thresholds 10 HU, 50 HU, 150 HU, 300 HU, and 600 HU, respectively. The total file sizes of the original image (not compressed) were 40.3MB, 2.38 MB, 1.56 MB, 846 KB, 658 KB and 401 KB (each down-scaled and compressed object) under these conditions. Therefore, we confirmed that the total image set size was approximately 1% of the original DICOM image set size when we used a down-scaled 3D object. It was confirmed through these results that the proper threshold decision process is a very important technique on this system.,

2) The transmission time for the down-scaled 3D object, when compared with the original transmission time, decreased to 9.54 %, 7.14 %, 3.62 %, 2.81 %, and 1.59 % under compressed conditions for the thresholds 10 HU, 50 HU, 150 HU, 300 HU, and 600 HU, respectively. The average transmission speed was 63.63 Kbps, and the transmission times were 359.49 sec (original image), 34.29 sec, 25.67 sec, 13.02 sec, 10.11 sec, and 5.71 sec (each down-scaled object) under these conditions. Therefore, we confirmed that the total transmission time was approximately 1.59% of the original DICOM image set when we used a down-scaled 3D object.

3) The proposed technique will become useful in supporting diagnosis for home and hospital care with additional studies. For example, the application range and efficiency of proposed technique will increase through the development of image transmission technique, security solution, image compression technique, object building technique, and 2D image reconstruction technique. In conclusion, the proposed technique will be helpful for e-Health network as a simple diagnostic method when it is connected with mobile and network technologies.

REFERENCES

[1] J. Kim, D. Feng, T. Cai, and S. Eberl, *"Content Access and Distribution of Multimedia Medical Data in E-health"*, ICME 2002, IEEE International Conference on Multimedia and Expo, pp.341-344, 2002.

[2] J. Zhang, J. N. Stahl, H. K. Huang, X. Zhou, S. L. Lou, and K. S. Song, *"Real-time teleconsultation with high-resolution and large-volume medical images for collaborative healthcare"*, IEEE transactions on information technology in Biomedicine , Vol. 4, pp.178 - 185, 2000.

[3] E. J. G´omez, F. D. Pozo, E. J. Ortiz, N. Malpica, and H. Rahms, *"A Broadband Multimedia Collaborative System for Advanced Teleradiology and Medical Imaging Diagnosis"*, IEEE transactions on information technology in Biomedicine, Vol. 2, No. 3, 1998.

[4] U. Engelmann, A. Schroter, U. Baur, O. Werner, M. Schwab, H. Mull, and H. Meinzer, *"A three-generation model for teleradiology"*, IEEE transactions on information technology in Biomedicine, Vol. 2, pp.20 - 25, 1998.

[5] S. A. Pavlopoulos, and A. N. Delopoulos, *"Designing and implementing the transition to a fully digital hospital"*, IEEE transactions on information technology in Biomedicine, Vol. 3, No. 1, pp.6-19, 1999.

[6] S. Hludov, Chr. Meinel, G. Norllr, and F. Warda, *"PACS for Teleradiology"*, 12th IEEE Symposium on Computer-Based Medical Systems, 1999.

[7] S. C. Hwang, and M. H. Lee, *"A WEB-Based TelePACS Using an Asymmetric Satellite System"*, IEEE transactions on information technology in Biomedicine, Vol. 4, 2000.

[8] H. J. Kim, H. M. Kim, S. W. Choi, S. J. Kim, T. S. Kim, Y. M. Son, and H. H. Lee, *"Development of Web-based DICOM image retrieval system"*, The 4th Asia-Pacific Conference on medical & biological engineering: Biomedical engineering for the 21st century, 1999.

[9] S. C. Hwang, J. W. Lee, J. H. Kim, I. K. Choi, G. S. Shin, H. J. Kim, and M. H. Lee, *"Development of WWW-Based TelePACS Using Satellite Data Communication"*, 20th Annual International conference of the IEEE Engineering in Medicine and Biology Society, 1998.

[10] A. B. Waluyo, R. Hsieh, D. Taniar, W. Rahayu, and B. Srinivasan, *"Utilising Push and Pull Mechanism in Wireless e-Health Enviroment"*, IEEE International Conference on e-Technology, e-Commerce and e-Service, 2004.

[11] LG. Yamamoto, *"Using JPEG image compression to facilitate telemedicine"*, Am J Emerg Med, Vol. 13, pp. 55-57, 1995.

[12] A. M. Bruckstein, M. Elad, and R. Kimmel, *"Down-Scaling for Better Transform Compression"*, IEEE transactions on image processing, Vol. 12, No. 9, pp.1132-1144, 2003.

[13] M. Hashimoto, K. Matsuo, A. Koike, and Y. Nakajima, *"Hierarchical structure for data transmission of volumetric medical images using three-dimensional wavelet transform"*, Nuclear Science Symposium Conference Record of IEEE, Vol. 3, No. 4-10, pp.1399-1403, 2001.